

## A 4-HYDROXY-1,8-NAPHTHALIMIDE-BASED TURN-ON TWO-PHOTON FLUORESCENT PROBE FOR HYDROGEN POLYSULFIDE SENSING

L. Zhou<sup>1,2,3\*</sup>, G. Yuan<sup>2</sup>, Sh. Hu<sup>1</sup>

<sup>1</sup> College of Life Sciences and Chemistry, Hunan University of Technology, Hunan 412007, China; e-mail: zhouly0817@163.com

<sup>2</sup> College of Food Science and Technology, Central South University of Forestry and Technology, Hunan 410004, China

<sup>3</sup> Hunan University, State Key Laboratory for Chemo/Biosensing and Chemometrics, Hunan 410082, China

In order to quantitatively detect hydrogen polysulfides ( $H_2S_n$ ,  $n > 1$ ) in biosystems, we propose a new two-photon turn-on fluorescent probe, named  $N_p-S_n$ , based on the D- $\pi$ -A skeleton two-photon fluorophore of 4-hydroxy-1,8-naphthalimide derivative and deprotection of 2-fluoro-5-nitrobenzoic ester by  $H_2S_n$ .  $N_p-S_n$  displayed a more than 80-fold enhancement towards  $H_2S_n$  in 550 nm and high sensitivity with a detection limit as low as 33 nM. Additionally, the probe  $N_p-S_n$  was further used for fluorescence imaging of  $H_2S_n$  in living cells under two-photon excitation (820 nm), which showed a high-resolution imaging, thus demonstrating its practical application in biological systems for the study of physiological and pathological functions of  $H_2S_n$ .

**Keywords:** hydrogen polysulfides, two-photon fluorescent imaging.

## ДВУХФОТОННЫЙ ФЛУОРЕСЦЕНТНЫЙ ЗОНД НА ОСНОВЕ 4-ГИДРОКСИ-1,8-НАФТАЛИМИДА ДЛЯ ОПРЕДЕЛЕНИЯ ПОЛИСУЛЬФИДА ВОДОРОДА

L. Zhou<sup>1,2,3\*</sup>, G. Yuan<sup>2</sup>, Sh. Hu<sup>1</sup>

УДК 535.372;621.317.729.2

<sup>1</sup> Колледж естественных наук и химии, Технологический университет Хунань, Хунань 412007, Китай; e-mail: zhouly0817@163.com

<sup>2</sup> Колледж пищевой науки и технологии, Южно-центральный лесотехнический университет, Хунань 410004, Китай

<sup>3</sup> Университет Хунань, Хунань, 410082, Китай

(Поступила 2 октября 2018)

Для количественного обнаружения полисульфида водорода ( $H_2S_n$ ,  $n > 1$ ) в биосистемах предложен двухфотонный флуоресцентный зонд  $N_p-S_n$  на основе структуры D- $\pi$ -A двухфотонного флуорофора — производного 4-гидрокси-1,8-нафталимида и 2-фтор-5-нитробензойной кислоты  $H_2S_n$ . Зонд  $N_p-S_n$  продемонстрировал более чем 80-кратное усиление флуоресценции при 550 нм по сравнению с  $H_2S_n$  и высокую чувствительность с пределом обнаружения 33 нМ. Он используется для флуоресцентной визуализации  $H_2S_n$  в живых клетках при двухфотонном возбуждении (820 нм).

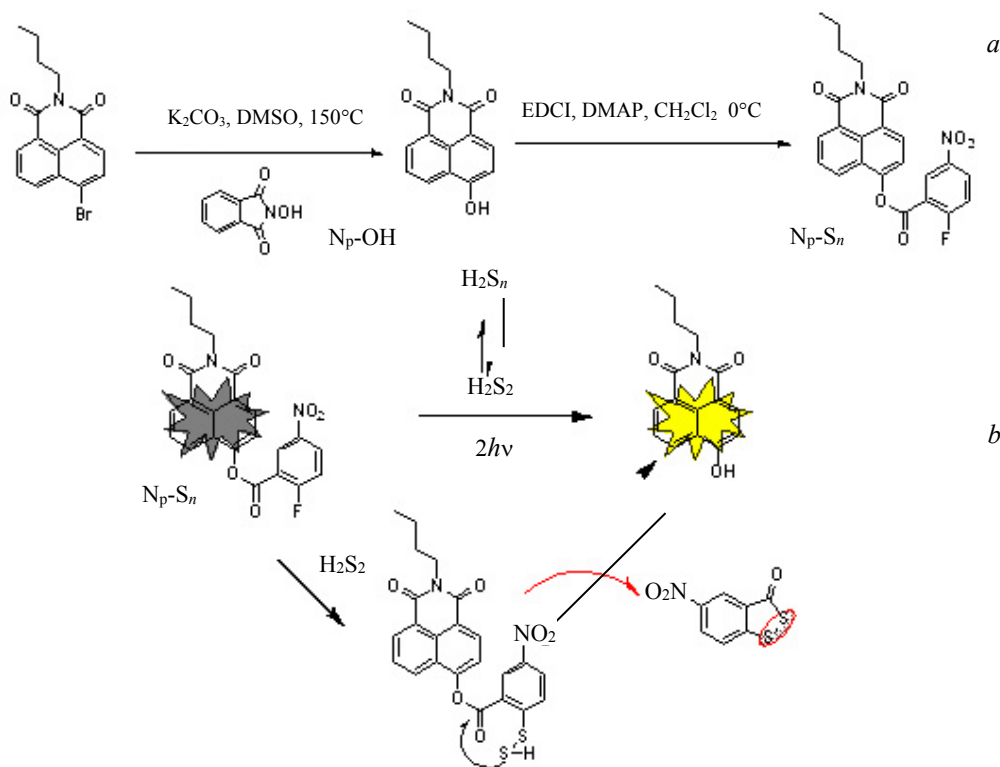
**Ключевые слова:** полисульфиды водорода, двухфотонная флуоресцентная визуализация.

**Introduction.** It is essential to detect endogenous substances in diagnosing disease. The performance of reactive sulfur species (RSS), including bio-thiols, hydrogen sulfide ( $H_2S$ ), hydrogen polysulfides ( $H_2S_n$ ,  $n > 1$ ), persulfides, and S-modified cysteine adducts (i.e., S-nitroso-thiols, sulfenic acids, etc.), is involved in every aspect of cell biology, from protein function to redox signal transduction [1, 2]. Among them,  $H_2S_n$ , which can be derived from endogenous  $H_2S$  by the action of reactive oxygen species, have recently received

particular attention since they are believed to be involved in  $\text{H}_2\text{S}$ -mediated signaling transduction [3]. As the redox partners of  $\text{H}_2\text{S}$ ,  $\text{H}_2\text{S}_n$  very likely coexist with  $\text{H}_2\text{S}$  *in vivo*, and they work together to regulate the sulfur redox balance. Recent studies suggested that  $\text{H}_2\text{S}_n$  might act as the real regulators in cellular signaling transduction. Some biological mechanisms previously attributed to  $\text{H}_2\text{S}$  may actually be mediated by  $\text{H}_2\text{S}_n$ . For instance,  $\text{H}_2\text{S}_n$  has recently been found to be more effective than  $\text{H}_2\text{S}$  in the conversion of protein cysteine residues (-SH) to persulfides (-S-SH) (S-sulfhydration) [4–6].

The investigation of  $\text{H}_2\text{S}_n$  is now rapidly increasing, and the biological activity mediated by  $\text{H}_2\text{S}_n$  is yet to be discovered [7–9]. In order to better understand the roles of  $\text{H}_2\text{S}_n$  in biosystems, it is critical to develop efficient methods that can distinguish  $\text{H}_2\text{S}_n$  from other RSS, especially  $\text{H}_2\text{S}$  and biothiols. The traditional method for detecting  $\text{H}_2\text{S}_n$  is to measure UV absorption peaks at 290–300 and 370 nm [10]. However, this detection method requires the reduction of polysulfides to  $\text{H}_2\text{S}$ . Due to this limitation, the traditional method cannot meet the demands of biological *in situ* detection in sensitivity and selectivity. Fluorescence-based methods could be ideal due to their rapid, sensitive fluorescent responses and spatiotemporal resolution capability. The unique chemical characteristics of sulfur species have been utilized in fluorescent probe design. For example,  $\text{H}_2\text{S}_n$  with the estimated  $\text{pK}_a$  values in the range from 3 to 5, are more acidic and nucleophilic than the corresponding  $\text{H}_2\text{S}$  (7.0) and thiols (Cys, 8.30; GSH, 9.20) due to the  $\alpha$ -effect under physiological pH. Compared with them, fluorescence-based methods could maintain comparable efficiency and accuracy, offer convenience and high sensitivity, as well as obtain noninvasive spatial temporal resolution imaging. Especially, two-photon (TP) probe-based fluorescent imaging, which is an emerging technique employing near-infrared (NIR) light source excitation that can provide improved spatial resolution and theoretically remarkably increased imaging depth in comparison with traditional one-photon (OP) imaging, might be the most attractive one for *in vivo* detection of bio-related species [11, 12]. Recently, some types of  $\text{H}_2\text{S}_n$  fluorescent probes have been developed by Xian [13–16] and others [17–21]. However, most of these fluorescent probes are OP fluorescent probes, and an effective two-photon fluorescent probe to specifically detect  $\text{H}_2\text{S}_n$  is very rare. Therefore, developing a simple and reliable TP fluorescent probe for the quantitative detection of  $\text{H}_2\text{S}_n$  concentration in living cells is of great interest.

Herein, we employed a large TP action absorption cross-section, high fluorescence quantum yield, excellent biocompatibility, and low fluorescence background fluorophore (4-hydroxy-1,8-naphthalimide) to design and synthesize a new TP turn-on fluorescent probe,  $\text{N}_p\text{-S}_n$ , for detecting  $\text{H}_2\text{S}_n$  (Scheme 1).



Scheme 1. The synthetic route of the fluorescent probe  $\text{N}_p\text{-S}_n$  and its reaction mechanism with  $\text{H}_2\text{S}_2$ .

The fluorescence intensity was quenched by the 2-fluoro-5-nitrobenzoic ester moiety through suppressing the intramolecular charge transfer (ICT) effect. Upon addition of  $\text{H}_2\text{S}_n$ , the 2-fluoro-5-nitrobenzoic ester moiety was cut off to form the OH group, resulting in the recovery of the ICT effect to turn on the fluorescence signal.  $\text{N}_p\text{-S}_n$ , exhibited a more than 80-fold fluorescence intensity enhancement at an emission wavelength of 550 nm after reaction with  $\text{H}_2\text{S}_n$ . Most importantly, the fluorescent probe exhibited high sensitivity and high selectivity toward  $\text{H}_2\text{S}_n$  over other analytes. Subsequently the probe was successfully applied to the detection of  $\text{H}_2\text{S}_n$  for bioimaging with a high-resolution imaging.

**Experiment.** Unless otherwise noted, all chemical reagents are supplied by commercial suppliers and used without further purification. All solvents were dried in a routine way and redistilled before use, and all water used in all experiments was secondarily distilled and purified by a Milli-Q system (Millipore, USA). Mass spectra were carried out by an LCQ Advantage ion trap mass spectrometer (Thermo Finnigan). NMR spectrum were recorded on a Bruker DRX-400 spectrometer in  $\text{DMSO-}d_6$  with TMS as the internal reference. All chemical shifts are reported in the standard  $\delta$  notation of parts per million. Absorption spectra were recorded in 1.0 cm path length quartz cuvettes on a Hitachi U-4100 UV-vis spectrophotometer (Kyoto, Japan). All fluorescence measurements were carried out on a F-4600 fluorescence spectrometer with both excitation and emission slits fixed at 2.5 nm. Fluorescence imaging of HeLa cells and tissues was conducted on a confocal laser scanning microscope (Olympus, Japan) with 820 nm excitation. Reactions were followed by thin-layer chromatography (TLC) on Merck (0.25 mm) glass-packed precoated silica gel plates (60 F254) and then visualized with a UV lamp. All chemical yields are unoptimized and generally represent the result of a single experiment. The pH was measured with a Mettler-Toledo Delta 320 pH meter.

*Synthesis and characterization of 2-butyl-6-hydroxy-1H-benzo[de]isoquinoline-1,3(2H)-dione (compound 2).* A 0.332 g (1.00 mmol) portion of 6-bromo-2-butyl-1H-benzo[de]isoquinoline-1,3(2H)-dione (**1**), 0.326 g N-Hydroxyphthalimide (2.00 mmol), 0.556 g (4 mmol)  $\text{K}_2\text{CO}_3$ , and 50 mL DMSO were added into a 100 mL flask with a reflux condenser, and the mixture was stirred at 150°C for 4 h under argon protection. Then the mixture was poured into ice water and filtered. Finally, the filtrate was dried in a vacuum oven to yield **2** as a yellow solid (0.243g, 90.1%).  $^1\text{H}$  NMR (400 MHz,  $d_6$ -DMSO)  $\delta$ : 8.55–8.53 (d,  $J$  = 8 Hz, 1H), 8.45–8.43 (d,  $J$  = 8 Hz, 1H), 8.31–8.23 (m, 1H), 7.71–7.67 (t,  $J$  = 8 Hz, 1H), 7.03–7.01 (d,  $J$  = 8 Hz, 1H), 5.76 (s, 1H), 4.04–4.0 (t,  $J$  = 8 Hz, 2H), 1.63–1.29 (m, 4H), 0.94–0.91 (t,  $J$  = 6 Hz, 3H);  $^{13}\text{C}$  NMR (100 MHz,  $d_6$ -DMSO)  $\delta$ : 164.36, 163.35, 134.38, 131.38, 130.20, 129.79, 125.20, 123.84, 122.21, 111.17, 55.27, 30.28, 20.47, 14.28; ESI-MS:  $[\text{M}]^+$  calcd: 269.30, found: 269.4.

*Synthesis and characterization of 2-butyl-1,3-dioxo-2,3-dihydro-1H-benzo[de]isoquinolin-6-yl 2-fluoro-5-nitrobenzoate ( $\text{N}_p\text{-S}_n$ ).* Compound **2** (0.135 g, 0.5 mmol), 2-fluoro-5-nitrobenzoic acid (0.0930 g, 0.5 mmol), 1-ethyl-(3-dimethylaminopropyl)carbodiimide hydrochloride (EDCI) (0.0960 g, 0.5 mmol), and 4-dimethylaminopyridine (DMAP) (0.0244 g, 0.2 mmol) were dissolved in dichloromethane (DCM) (40 mL) under argon protection at 25°C for 12 h. Then, the mixture was poured into ice water and extracted three times by DCM (15 $\times$ ). Then, the solvent was evaporated in vacuum, and the crude solid was purified by column chromatography on silica gel eluting ( $\text{CH}_2\text{Cl}_2/\text{MeOH}$  = 100:1, v/v) to afford a 0.198g yellow solid in 90.4% yield.  $^1\text{H}$  NMR (400 MHz,  $d_6$ -DMSO)  $\delta$ : 8.95 (s, 1H), 8.88 (s, 1H), 8.69–8.67 (t,  $J$  = 4 Hz, 1H), 8.57–8.49 (m, 3H), 7.93–7.88 (q,  $J$  = 10 Hz, 2H), 7.84–7.79 (t,  $J$  = 10 Hz, 1H), 4.06–4.02 (t,  $J$  = 8 Hz, 2H), 1.64–1.320 (m, 4H), 0.95–0.92 (t,  $J$  = 6 Hz, 3H);  $^{13}\text{C}$  NMR (100 MHz,  $d_6$ -DMSO)  $\delta$ : 166.62, 163.91, 163.64, 163.12, 160.43, 151.09, 144.31, 131.76, 128.98, 128.64, 128.40, 125.04, 122.88, 121.01, 120.64, 119.92, 119.67, 118.68, 118.57, 30.08, 20.27, 14.18; ESI-MS:  $[\text{M}]^+$  calcd: 436.40, found: 436.4.

The fluorescence was measured in a 10 mM phosphate buffer solution (containing 1% DMSO as a co-solvent). The pH value of the PBS solution used was from 4.0 to 9.0, which was achieved by adding minimal volumes of the HCl solution or the NaOH solution. The fluorescent emission spectra were recorded at an excitation wavelength of 400 nm with emission wavelength range from 520 to 630 nm. A  $1 \times 10^{-3}$  mol/L stock solution of the probe was prepared by dissolving  $\text{N}_p\text{-S}_n$  in DMSO. The procedure of calibration measurements with the probe in the buffer with different  $\text{H}_2\text{S}_n$  followed: 2  $\mu\text{L}$  stock solution of the probe and 1998  $\mu\text{L}$  of the PBS buffer solution with different  $\text{H}_2\text{S}_n$  were combined to afford a test solution, which contained  $1 \times 10^{-6}$  mol/L of probe. The solutions of various testing species were prepared from 0.5 mM Cys, 0.5 mM Hcy, 0.5 mM GSH, 0.5 mM CysSSCys, 0.5 mM GSSG, 0.5 mM Cys-poly-sulfide, 0.5 mM  $\text{S}_8$ , 20  $\mu\text{M}$   $\text{Na}_2\text{S}_2$ , 0.5 mM  $\text{NaHSO}_3$ , 0.5 mM ascorbic acid, 0.5 mM tocopherol, 0.5 mM NaHS, and 0.5 mM  $\text{Na}_2\text{S}_2\text{O}_3$ . The procedure of the selectivity experiments consists of  $1 \times 10^{-6}$  mol/L of the probe and different concentrations of analytes.  $\text{Na}_2\text{S}_2$  was prepared using the reported procedures [14]. The mixture was equilibrated for 5 min before measurement.

Prior to the image experiments, the HeLa cells were washed with phosphate-buffered saline (PBS), and incubated with 1  $\mu\text{M}$  probe  $\text{N}_p\text{-S}_n$  for 30 min at 37°C, then washed with PBS three times and incubated with 15  $\mu\text{M}$   $\text{Na}_2\text{S}_2$  for another 30 min at 37°C. Finally, the HeLa cells were washed with PBS three times again before imaging. A confocal fluorescence image of  $\text{H}_2\text{S}_2$  in HeLa cells was observed under an Olympus FV 1000 laser confocal microscope. Two-photon image:  $\lambda_{\text{ex}} = 820$  nm,  $\lambda_{\text{em}} = 500\text{--}570$  nm. All images were acquired with a 40 $\times$  oil immersion objective, scale bar 10  $\mu\text{m}$ .

**Results and discussion.** As a proof of concept, a D- $\pi$ -A-structured  $\text{N}_p\text{-S}_n$  was chosen as the fluorophore for its outstanding two-photon properties, while a 2-fluoro-5-nitrobenzoic ester moiety was used as the recognition moiety due to its rapid response to  $\text{H}_2\text{S}_2$ , according to some reports [17–21]. All compounds were characterized by  $^1\text{H}$  and  $^{13}\text{C}$  NMR and ESI-MS.

As expected, the spectroscopic properties of  $\text{N}_p\text{-S}_n$  (1  $\mu\text{M}$ ) were examined in a phosphate buffer solution (10 mM, pH 7.4) with different concentrations of  $\text{Na}_2\text{S}_2$ . The probe displays sensitive absorption and fluorescence responses to different concentrations of  $\text{Na}_2\text{S}_2$  (Fig. 1). As shown in Fig. 1a, in the absence of  $\text{Na}_2\text{S}_2$ , an absorption peak was observed at the maximum absorption wavelengths  $\lambda = 350$  nm. After  $\text{Na}_2\text{S}_2$  (15  $\mu\text{M}$ ) was added, two absorption peaks were observed at the maximum absorption wavelengths  $\lambda = 350$  and 475 nm. Further fluorescence experiments showed that  $\text{N}_p\text{-S}_n$  is weakly-fluorescence (Fig. 1b) due to the strong electron-withdrawing 2-fluoro-5-nitrobenzoic ester moiety that prevented the  $\text{N}_p\text{-S}_n$  from changing to fluorophore  $\text{N}_p\text{-OH}$ . Upon reaction with  $\text{Na}_2\text{S}_2$  from 0 to 25  $\mu\text{M}$ , which results in converting into  $\text{N}_p\text{-OH}$  and a significant turn-on fluorescence enhancement at  $\lambda_{\text{em}} = 550$  nm, the fluorescence ratio of  $F_{550}/F_0$  gradually increased  $\sim 80$ -fold. Further detailed studies also revealed that there is an excellent linear relationship between  $F_{550}$  and different  $\text{Na}_2\text{S}_2$  concentrations (0–5.0  $\mu\text{M}$ ) (Fig. 1c). The detection limit (utilizing the  $3\sigma/k$  method) for  $\text{H}_2\text{S}_2$  was determined to be as low as 33 nM, which is enough for direct detection of  $\text{H}_2\text{S}_2$  *in vitro* and *in vivo*.

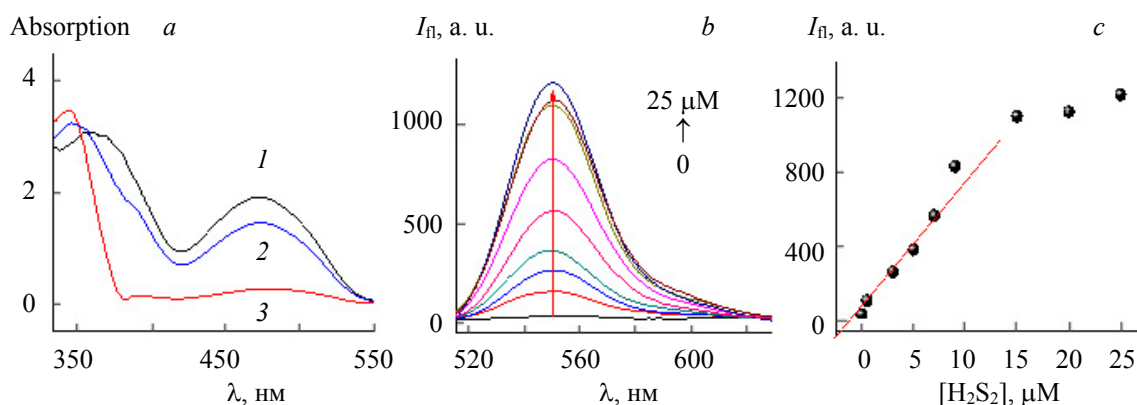


Fig. 1. (a) UV-vis absorption (1): 1  $\mu\text{M}$   $\text{N}_p\text{-OH}$ ; (2): 1  $\mu\text{M}$   $\text{N}_p\text{-S}_n$ +15 $\mu\text{M}$   $\text{Na}_2\text{S}_2$ ; (3): 1 $\mu\text{M}$   $\text{N}_p\text{-S}_n$ ; (b) fluorescence spectra of  $\text{N}_p\text{-S}_n$  1  $\mu\text{M}$  in the presence of various concentrations of  $\text{Na}_2\text{S}_2$  (0–25  $\mu\text{M}$ ); (c) calibration curve of  $\text{N}_p\text{-S}_n$  to  $\text{Na}_2\text{S}_2$ . The curve was plotted with fluorescence intensity vs  $\text{Na}_2\text{S}_2$  concentration (0–25  $\mu\text{M}$ ).

Naphthalimide derivatives exhibit excellent two-photon properties with a two-photon action cross-section, showing that this two-photon dye is potentially useful for bioimaging applications. The  $\text{N}_p\text{-S}_n$  was calculated to have a two-photon absorption cross-section of 12 GM (1 GM =  $10^{-50}$   $\text{cm}^4 \cdot \text{s}/\text{photon}$ ) at 550 nm upon excitation at 820 nm (Fig. 2a, curve 2). However, the  $\text{N}_p\text{-OH}$  was calculated to have a large two-photon absorption cross-section of 78 GM, as well as a new strong fluorescent peak at 550 nm (curve 1). High selectivity is an important parameter to evaluate a newly designed fluorescent probe. For this purpose,  $\text{N}_p\text{-S}_n$  was treated with a series of analytes such as Cys, Hcy, GSH, CysSSCys, GSSG, Cys-poly-sulfide,  $\text{S}_8$ ,  $\text{Na}_2\text{S}_2$ ,  $\text{NaHSO}_3$ , ascorbic acid, tocopherol,  $\text{NaHS}$ , and  $\text{Na}_2\text{S}_2\text{O}_3$  to examine its selectivity. The results are shown in Fig. 2b. The probe demonstrated almost unchanged fluorescence intensity responses before and after addition of analytes to the  $\text{N}_p\text{-S}_n$  solution.  $\text{N}_p\text{-S}_n$  could meet the selective requirements for practical applications. Next, we studied the effect of the pH on  $\text{N}_p\text{-S}_n$  in the absence and presence of  $\text{H}_2\text{S}_2$  (Fig. 2c). Without  $\text{H}_2\text{S}_2$ , no obvious characteristic fluorescence could be observed from pH 3.0–9.0 (Fig. 2c, curve 2). Upon reaction with  $\text{H}_2\text{S}_2$ , the best response towards  $\text{H}_2\text{S}_2$  could be achieved with a pH range of 4.0–8.0 (Fig. 2c, curve 1).

Thus, the PBS solution (pH 7.4) was utilized throughout the experiment. These results indicated  $N_p-S_n$  was favorable for applications in practical samples at different pH values.

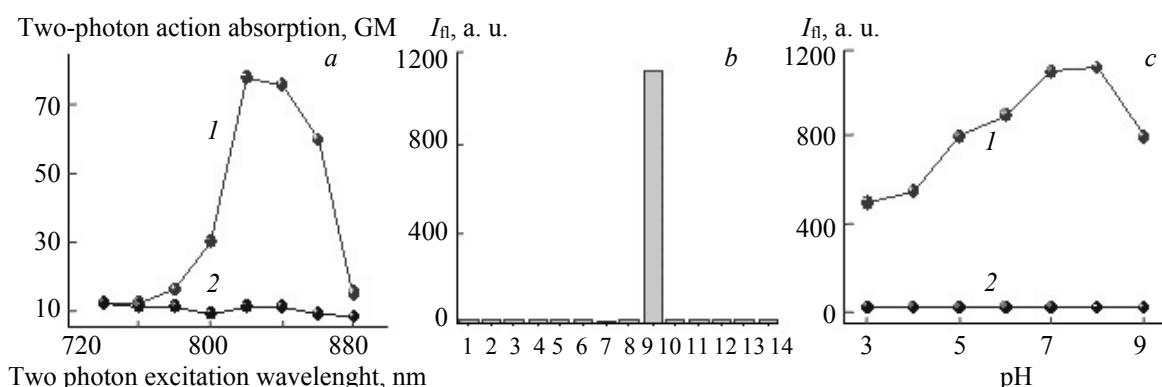


Fig. 2. (a) Two-photon absorption cross-section of  $N_p-OH$  (1) and  $N_p-S_n$  (2); (b) fluorescence responses of  $N_p-S_n$  ( $1 \mu M$ ) to biologically relevant RSS. Numbers from 1 to 14 correspond to black to  $Na_2S_2O_3$  (blank, 0.5 mM Cys, 0.5 mM Hcy, 0.5 mM GSH, 0.5 mM CysSSCys, 0.5 mM GSSG, 0.5 mM Cys-poly-sulfide, 0.5 mM  $S_8$ , 20  $\mu M$   $Na_2S_2$ , 0.5 mM  $NaHSO_3$ , 0.5 mM ascorbic acid, 0.5 mM tocopherol, 0.5 mM NaHS, and 0.5 mM  $Na_2S_2O_3$ ); (c) pH effects on  $N_p-S_n$  (1) in the absence or presence of  $Na_2S_2$  (2). Data were recorded in 10 mM PBS buffer (pH 7.40, containing 5% DMSO as a cosolvent) at room temperature for 5 min.  $\lambda_{ex} = 475$  nm,  $\lambda_{em} = 550$  nm.

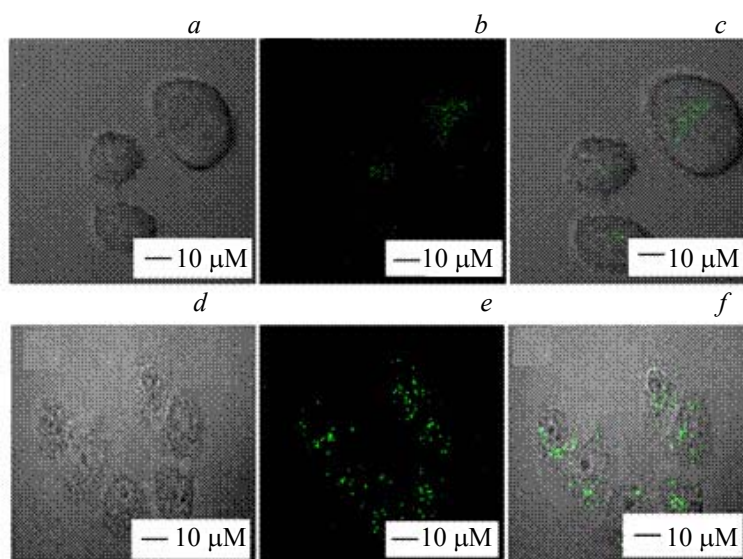


Fig. 3. TP fluorescence microscope (TPFM) images of HeLa cells: (a) bright field image; (b) HeLa cells incubated with  $1 \mu M$   $N_p-S_n$  for 30 min; (c) merged image of (b) and bright field image (a); (d) bright field image; (e) HeLa cells pretreated with  $10 \mu M$   $Na_2S_2$  for 15 min and then incubated with  $1 \mu M$   $N_p-S_n$  for 30 min image; (f) merged image of (e) and bright field image (d). TP images:  $\lambda_{ex} = 820$  nm,  $\lambda_{em} = 500-570$  nm. All images were acquired with a  $40\times$  oil immersion objective, scale bar  $10 \mu m$ .

In order to evaluate the imaging performance of  $N_p-S_n$ , we used this probe to detect  $H_2S_2$  in live cells. HeLa cells were chosen as the model cell line. Before imaging, the cytotoxicity of the  $H_2S_2$  was tested. The results showed that it was nearly nontoxic for living cells under experimental conditions. Then the HeLa cells were incubated with  $N_p-S_n$  ( $1 \mu M$ ) at  $37^\circ C$  for 30 min, followed by excitation at 820 nm for TP image. The HeLa cells showed a weak fluorescence intensity in the green channel by TP image (Fig. 3b). In contrast, when treating  $N_p-S_n$ -incubated cultured cells with  $10 \mu M$   $Na_2S_2$  for 30 min, the fluorescence intensity increased in the green channel, obviously (Fig. 3e) by TP image. Taken together, these results showed that  $N_p-S_n$  was cell membrane-penetrable and could be used for TP images in live cells.

**Conclusion.** We designed and synthesized a novel TP fluorescent probe  $N_p-S_n$  to detect  $H_2S_n$  in living cells and tissues. The probe is based on TP excitation of the D- $\pi$ -A structure of 4-hydroxy-1,8-naphthalimide derivative fluorophore ( $N_p-OH$ ), which is obtained upon removal of a trigger moiety by the  $H_2S_n$  of interest. The probe was demonstrated to efficiently image  $H_2S_n$  produced in live cells. We believe that the probe  $N_p-S_n$  will be a useful tool for the study of physiological and pathological functions of  $H_2S_n$  in biological systems.

**Acknowledgment.** This work was supported by the National Natural Science Foundation of China (Grants 21605046) and the Natural Science Foundation of Hunan Province (Grants 2017JJ3060).

The authors declare no conflicts of interest.

## REFERENCES

1. G. I. Giles, K. M. Tasker, C. Jacob, *Free Rad. Biol. Med.*, **31**, 1279–1283 (2001).
2. M.C. H. Gruhlke, A. J. Slusarenko, *Plant Physiol. Biochem.*, **59**, 98–107 (2012).
3. P. Nagy, M. T. Ashby, *J. Am. Chem. Soc.*, **129**, 14082–14091 (2007).
4. C. E. Paulsen, K. S. Carroll, *Chem. Rev.*, **113**, 4633–4679 (2013).
5. D. Zhang, I. Macinkovic, N. O. Devarie-Baez, J. Pan, C. M. Park, K. S. Carroll, M. R. Filipovic, M. Xian, *Angew. Chem. Int. Ed.*, **53**, 575–581 (2014).
6. H. Kimura, *Nitric Oxide*, **41**, 4–10 (2014).
7. P. Nagy, Z. Pálincás, A. Nagy, B. Budai, I. Tóth, A. Vasas, *Biochim. Biophys. Acta: Gen. Subjects*, **1840**, 876–891 (2014).
8. O. Kabil, N. Motl, R. Banerjee, *Biochim. Biophys. Acta: Proteins Proteomics*, **1844**, 1355–1366 (2014).
9. H. Kimura, *Neurochem. Int.*, **63**, 492–497 (2013).
10. R. Greiner, Z. Pálincás, K. Bäsell, D. Becher, H. Antelmann, P. Nagy, T. P. Dick, *Antioxid. Redox Signal.*, **19**, 1749–1765 (2013).
11. H. M. Kim, B. R. Cho, *Chem. Asian J.*, **6**, 58–69 (2011).
12. H. M. Kim, B. R. Cho, *Acc. Chem. Res.*, **42**, 863–872 (2009).
13. W. Chen, E. W. Rosser, D. Zhang, W. Shi, Y. Li, W. Dong, H. Ma, D. Hu, M. Xian, *Org. Lett.*, **17**, 2776–2779 (2015).
14. W. Chen, C. Liu, B. Peng, Y. Zhao, A. Pacheco, M. Xian, *Chem. Sci.*, **4**, 2892–2896 (2013).
15. W. Chen, E. W. Rosser, T. Matsunaga, A. Pacheco, T. Akaike, M. Xian, *Angew. Chem. Int. Ed.*, **54**, 13961–13965 (2015).
16. C. Liu, W. Chen, W. Shi, B. Peng, Y. Zhao, H. Ma, M. Xian, *J. Am. Chem. Soc.*, **136**, 7257–7260 (2014).
17. L. Zeng, S. Chen, T. Xia, W. Hu, C. Li, Z. Liu, *Anal. Chem.*, **87**, 3004–3010 (2015).
18. Y. Huang, F. Yu, J. Wang, L. Chen, *Anal. Chem.*, **88**, 4122–4129 (2016).
19. Q. Han, Z. Mou, H. Wang, X. Tang, Z. Dong, L. Wang, X. Dong, W. Liu, *Anal. Chem.*, **88**, 7206–7212 (2016).
20. J. Zhang, X. Zhu, X. Hu, H. Liu, J. Li, L. Feng, X. Yin, X. Zhang, W. Tan, *Anal. Chem.*, **88**, 11892–11899 (2016).
21. H. Shang, H. Chen, Y. Tang, R. Guo, W. Lin, *Sensor Actuator B*, **230**, 773–778 (2016).